Multiple Fault Tolerant Measurement Based on Computational intelligent Techniques for a Continuous Stirred Tank Heater plant

Farouq Zargany, Mehdi Shahbazian, Houshang Jazayeri rad

Department of Automation and Instrumentation, Petroleum University of Technology, Ahvaz, Iran
Far.zargany@gmail.com

Abstract: A multiple fault tolerant measurement system based on nonlinear dynamic models, a special search algorithm, principle components decomposition and Q test is developed. The proposed system uses a model-based estimator to deliver symptoms. The symptoms are then analyzed in a statistical unit in order to detect the faults and isolate the faulty sensors. Multi-layer perceptron networks, radial basis function networks and Tagaki-Sugeno fuzzy models were examined for the fault estimator module while fuzzy models presented the best performance. The main advantages of the proposed scheme are the capability to detect, isolate and repair multiple faults in both input and output sensors and the feasibility to be applied to any system with as many sensors as required, all due to particular design of its model-based estimator. The system was tested on a CSTH model developed based on an experimental platform; different experiments demonstrated satisfactory results.

[Farouq Zargany, Mehdi Shahbazian, Houshang Jazayeri rad. **Multiple Fault Tolerant Measurement Based on Computational intelligent Techniques for a Continuous Stirred Tank Heater plant.** *J Am Sci* 2012;8(1s):9-18]. (ISSN: 1545-1003). http://www.jofamericanscience.org. 2

Key words: Multiple faults, fuzzy model, neural network, fault detection, fault isolation

1. Introduction

Nowadays increasing complexity of industrial plants necessitates reliable measurement systems that can minimize the operational risk and increase the system robustness in order to maintain the plant normal operation in the case of abnormal situations.

To detect any abnormality in the process operation two main approaches are applied: fault detection and identification (FDI) and fault detection and diagnosis (FDD). The former identifies the occurrence, type, location and time of the fault. The latter can identify all what FDI can as well as size and dynamic characteristics.

It is assumed that any kind of abnormality in the process behavior is due to a fault. Most of the fault detection approaches are based on residual generators that include analytical and functional redundancy or physical and hardware redundancy techniques. However, fault detection and diagnosis methods are not enough to guarantee the process normal operation after occurrence of a fault. Therefore, it is crucial to have a fault tolerant control system that can reconstruct the damaged signals and estimate the real signal.

Fault detection and isolation have received much attention in recent years. In [1] a physical redundancy approach is presented that detects the faults in measurement systems by applying simple statistical techniques. Also an analytical redundancy approach is introduced that detects the faults based on a linear model and least square analysis for the residuals. In this method a matrix that states the relationship between the quantities is required. Simani et al [2] suggest a fault detection system based on neural networks that employ an observer bank for residual generation. Neural networks are also used for fault classification. Described procedure shows good results for step-like faults, other faults have not been considered and it is not possible to reconstruct the damaged signal. Balle [3] applies a fuzzy modeling approach to detect sensor faults in a thermal platform. The scheme uses linear Tagaki-Sugeno fuzzy models to generate parity relations. The results indicate that the designed scheme can detect the faults in the five measurements under analysis. Edward and Alwi present a fault detection scheme based on sliding mode theory. The method requires

Information about which sensors are prone to faults and the results only show the faults in input sensors. Raoufi and Marquez [4] applied generalized sliding mode observers to estimate both input and output corrupted signals simultaneously. The scheme requires knowing which sensors are likely to fail. Du and Jin [5] used joint angle plots and multi-level principle component analysis to detect and isolate multiple faults. The reconstruction procedure is done based on a compensatory technique that finds the bias for a signal that minimizes the square prediction error. In this approach, the isolation process requires historical fault data to create a knowledge base.

The fact that losing a signal due to occurrence of a fault can extend to whole operation failure make it necessary to design and implement fault tolerant measurement systems that can provide corrected measurements in the presence of faults.

In this research work a new method is proposed to detect and diagnose sensor faults. The

presented scheme is designed to reconstruct the damaged signals using a simple reconstruction method creating a fault tolerant measurement system. The developed scheme combines the capabilities of both model based and statistical methods enabling the system to recognize sensor faults and reconstruct the faulty signals. The symptoms are generated using Tagaki-Sugeno fuzzy models which are obtained from an identification procedure. By combining statistical methods, a specific search algorithm, principle component analysis and Q test, sensor faults are detected and the faulty sensors are isolated. Finally a correction step is applied and the damaged signals are reconstructed.

The designed scheme was tested on 9 sensor measurement of an continuous stirred tank heater (CSTH) model. The model is based in an experimental platform in department of chemical engineering in IIT Bombay [6].

The paper is organized as it follows. The describes the CSTH platform and its basic equations. In the third section the scheme proposed to diagnose the faults and reconstruct the damaged signals is explicated and the main techniques are presented. The fourth section discusses different test scenarios and presents the obtained results and section 5 concludes the paper.

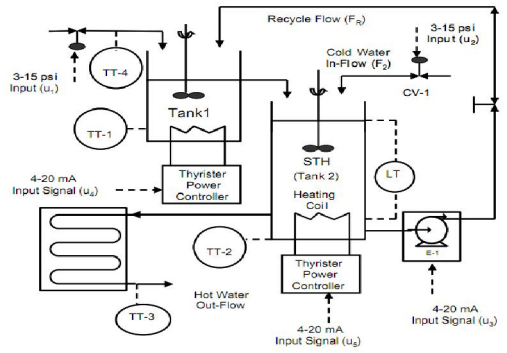

Fig. 1 The continuous stirred tank heater (CSTH) [6]

2.The Continuous Stirred Tank Heater (CSTH)

2.1. CSTH model description

An experimental platform of a CSTH has been developed in the automation laboratory of chemical engineering department in IIT Bombay [6,7]. Fig. 1 illustrates the process model. Cold water enters into tank 1 and tank 2 and it is heated using separate electric heaters in each tank. The hot water from tank 2 is recycled into tank 1 which introduces additional complexity into the process. The model involves five inputs: water flow rate into tank1, water flow rate into tank2, reverse flow rate from tank 2 to tank1, heat flow rate into tank 1, heat flow rate into tank 2 and four outputs: water temperature of tank1, water temperature of tank2, output flow from tank2 and water level of tank2. Table 1 presents the model parameters and units.

2.2. CSTH basic relations

Equations 1 and 2 are the dynamic heat balance equations of the plant and Equation 3 expresses the dynamic mass balance relationship.

$$V_1 \frac{dT_1}{dt} = F_1(T_C - T_1) + F_R(T_2 - T_1) + \frac{Q_1}{\rho C_p} \quad (1)$$

$$A_2 h_2 \frac{dT_2}{dt} = F_1(T_1 - T_2) + F_2(T_C - T_2) - F_R(T_2 - T_1) + \frac{1}{\rho C_p}[Q_2 - 2\pi r_2 h_2 U(T_2 - T_a)] \quad (2)$$

$$A_2 \frac{dh_2}{dt} = F_1 + F_2 - F_{out}(h_2) \quad (3)$$

The input heat and flow rates are functions of input variables $u_1,\ldots, u_5$ and the tank2 output flow rate is a function of level. Correlations have been fit for these parameters experimentally. The correlations are provided below:

$$F_{out}(h_2) = 0.1 \times 10^{-3} \times (0.406h_2^3 + 0.8061h_2^2 - 0.01798h_2 + 0.1054)^{\frac{1}{2}} \quad (4)$$

$$F_1(u_1) = (42379u_1 - 456.85u_1^2 + 8.0368u_1^3) \times 10^{-11} \quad (5)$$

$$F_2(u_2) = (196620u_2 - 8796.8u_2^2 + 190.64u_2^3 - 1.294u_2^2) \times 10^{-11} \quad (6)$$

$$F_R(u_3) = 2u_3(1/3600) \times 10^{-3} \quad (7)$$

$$Q_1(u_4) = 7.9798u_4 + 0.9893u_4^2 - 7.3 \times u_4^2 \quad (8)$$
$$-8 \times 10^{-3}u_5^3$$

$$Q_5(u_5) = 104 + 14.44u_5 + 0.96u_5^2 - 8 \times 10^{-3}u_5^3 \quad (9)$$

It is important to note that variables $u_1,\ldots, u_5$ in the above correlations are expressed in percent varying between 0 to 100%.

In this work, Simulink model of the described plant is developed in MATLAB environment based on dynamic heat and mass balance equations and the correlations stated above. The model is used in order to acquire data and perform the required experiments.

3.Fault detection and diagnosis system

Fault detection and diagnosis based on mathematical models have concentrated much attention in the last 20 years [8]. The conventional approach for model-based fault detection is to use a model or an observer to estimate different variables of a process. The most popular models are state space, auto regressive, neural networks and fuzzy models. These models can be linear or nonlinear [9-13].

The most common approach for sensor fault detection and diagnosis is to compare the process measurements with those obtained from a mathematical model; the difference between these two is referred to as residual. This approach is applied in [2, 14] for example. Different methods such as dedicated observers, parity relations and parameter identification [15] are used for residual

generation. After residual generation, a classification procedure is carried out in order to distinguish between faulty sensors and those operating at normal condition. Neural networks are very common in this context. In this approach although it is possible to detect the faults but it is difficult and sometimes impossible to rebuild the damaged signals. Recent research work in this context is concentrated on increasing system robustness in residual generation and residual classification steps [16-18].

Table 1. CSTH model parameters

V_1 *Volume of tank1*	$1.75 \times 10^{-3}\ m^3$
A_2 *Cross sectional area of tank2*	$7.85 \times 10^{-3}\ m^2$
r_2 *radius of tank2*	0.05 m
U *Heat transfer coefficient*	$235.1\ W/m^2K$
T_C *Cooling water temperature*	$30\ ^0C$
T_a *atmospheric temperature*	$25\ ^0C$
F_1 *tank1 input flow*	cm^3/s
F_2 *tank2 input flow*	cm^3/s
F_R *reverse flow from tank2 to tank1*	cm^3/s
F_{out} *tank2 output flow*	cm^3/s
Q_1 *tank1 input heat*	J/s
Q_2 *tank2 input heat*	J/s
T_1 *tank1 temperature*	^0C
T_2 *tank2 temperature*	^0C
h_2 *tank2 level*	*cm*

On the other hand, there are fault detection approaches that do not require a model, approaches based on statistical analysis are in this category [19-20]. However due to presence of disturbances that usually affect the process, strong restrictions should be considered for the process variables such as constant variance and constant mean. Another disadvantage of these algorithms is that although they can detect the faults, they hardly can identify the fault origin or reconstruct the damaged signals.

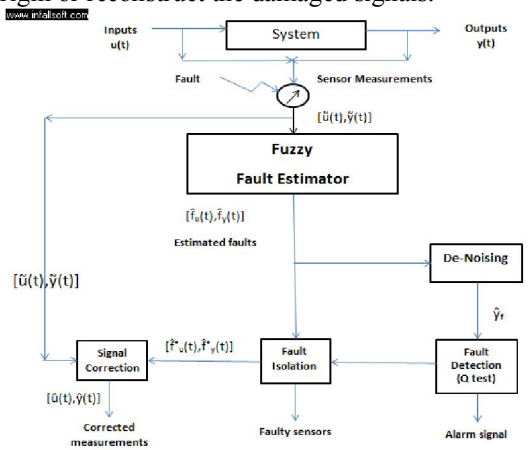

Fig. 2. The proposed multiple fault tolerant measurement scheme

3.1. Proposed scheme

The proposed scheme is presented in Fig. 2 in which the fault signals are estimated by the fault estimator directly. The scheme receives input and output sensor measurements as the input and provides fault alarm signal and faulty sensor or sensors as the output. As it is illustrated in Fig. 2 the scheme has 4 stages. In the first stage, faults are estimated by the fault estimator. In the second stage statistical methods (PCA and Q test) are applied to detect the presence of faults. In the third stage the faulty sensor is isolated and in the fourth stage the damaged signals are corrected.

The main purpose of this work is to integrate the capabilities of both model-based and statistical methods in order to increase the system robustness and improve its fault detection and diagnosis ability in the presence of noise and disturbance.

In this research, the faults are considered as additive faults in both input and output sensors. Therefore the faulty signals are considered as:

$$\begin{cases} \tilde{u}(t) = u(t) + f_u(t) \\ \tilde{y}(t) = y(t) + f_y(t) \end{cases} \quad (10)$$

Where u(t) and y(t) are the input and output sensor measurements in the absence of faults. The measurement signals $[\tilde{u}(t),\tilde{y}(t)]$ enter into the fault estimator that provides estimations of symptoms $[\hat{f}_u(t),\hat{f}_y(t)]$. It is expected to have a null vector of symptoms in the absence of faults but due to noise and modeling error, the estimator output is not null.

By comparing the estimated value of faults against a properly adjusted dynamic threshold, the faults are detected. Reconstruction of the damaged signals is completed by subtracting the fault estimations $[\hat{f}_u(t),\hat{f}_y(t)]$ from the sensor measurements $[\tilde{u}(t),\tilde{y}(t)]$.

3.2. Fault estimator and search algorithm

3.2.1. Fault estimator

In this work the fault estimator is a dynamic model that receives the sensor measurements as the input and delivers the fault signals as the output. By applying identification techniques to process data, the process modeling is accomplished which results in a model based fault estimator.

The model is defined as it is follows:

$$\widetilde{W}(t) = g(\tilde{\imath}(t)) \quad (11)$$

Where $\tilde{\imath}(t)$ is the vector of sensor measurements $[\tilde{u}(t), \tilde{y}(t)]$, $\widetilde{W}(t)$ is the vector of estimated faults $[\hat{f}_u(t),\hat{f}_y(t)]$ and g(•) is a nonlinear function. By applying dynamic modeling techniques, available data pairs $[\tilde{w}(t), \tilde{\imath}(t)]$ are employed to identify a data driven model in order to be used as nonlinear function g(•).

It is important to note that in order to obtain a reliable model that can provide symptoms with sufficient accuracy the following conditions must be held:

• Data should include the process operation under different operating points, steady states and transient situations.

• Data should be gathered when no internal fault acts on the process operation.

If the above conditions are held, fault detection and diagnosis become feasible, since the fault estimator is identified to deliver both input and output fault signals (symptoms).

For the fault estimator part of the system, Tagaki- Sugeno fuzzy models are utilized[21]. As it is illustrated in Fig.3 the T-S system consists of 5 layers. The nodes in the first layer determine the membership degree of each input. Nodes in the second layer are fixed and have the role of constant multipliers. Outputs of this layer provide the firing strength of rules and are denoted by W letter. Nodes in the third layer calculate the ratio of fifing strength of ith layer to the sum of firing strengths of all layers. The output of this layer is denoted by $\bar{W}$. The output of nodes in the fourth layer is the product of outputs of third layer with a linear model. Finally the fifth layer sums up all the incoming signals and calculates the output of the fuzzy model. The parameters of the first layer and fourth layer are adjustable parameters. A hybrid strategy including least squares and gradient descent optimization methods is employed to optimize these parameters. The gradient descent and least square methods are applied to first and fourth layers respectively. [22]

Mathematically, Tagaki-Sugeno (T-S) fuzzy models are constructed based on rules with the following definition [23]:

If x_1 is A_1^k and, …, and x_n is A_n^k then $y^k = g^k(\bullet)$ (12)

Where x_n is the nth input, A_n^k is the nth membership function in the kth rule and $g^k(\bullet)$ is a linear function with the following form:

$$g^k(\bullet) = b_0^k + b_1^k x_1 + \ldots + b_n^k x_n \quad (13)$$

Where x_n is the nth input and b_n is the nth constant.

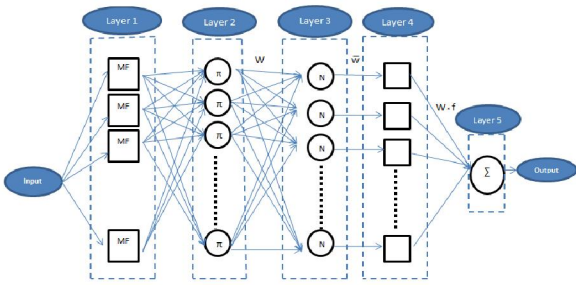

Fig. 3. Tagaki-Sugeno fuzzy model structure

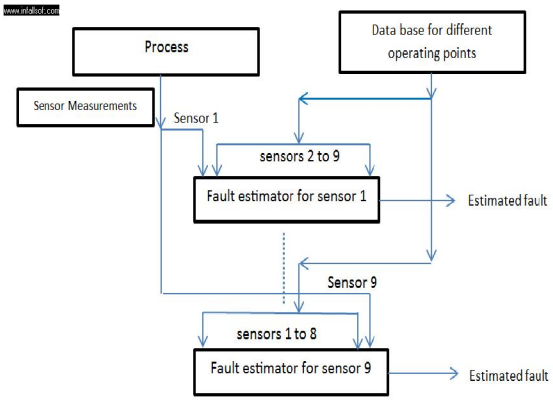

Fig.2. The proposed multiple fault tolerant measurement scheme

3.2.2 Search algorithm

Fig. 4 illustrates the the diagram of the procedure followed by a search algorithm which is augmented to the fault estimator in order to enable the estimator to detect multiple faults simultaneously. In this method data obtained from different operating points of the process are collected in a database. For every sensor in the process, an independent partition of the fault estimator is dedicated. Every partition of the fault estimator has 9 inputs and 1 output. 9 inputs correspond to 9 sensor measurements of the process and 1 output provides the estimated fault for the sensor under analysis. The search algorithm works in the following way: At every operating point of the process, the algorithm analyzes values of sensor measurement in order to find the operating point. The algorithm then imports one sensor measurement into the corresponding fault estimator partition. The 8 remaining inputs are imported from the database having normal data. Therefore when more than one sensor become faulty at the same moment every partition of the fault estimator detects the presence of fault in one sensor and as a result the system is able to detect multiple faults simultaneously.

3.3. Alternative models (12)

Perceptron networks: In this type of neural networks, the output of each neuron is computed as:

$$y_j = g\left(\sum_{i=1}^{k}(W_{j,k}\, x_k) - b_j\right) \quad (14)$$

In which x_k is the network's kth input variable, $W_{j,k}$ is the weight of kth input x_k for neuron j, and b_j is the bias for neuron j. sigmoidal function (g(•)) is the commonly used function in this kind of networks [23]. Fig. 5 illustrates the function of a neuron and the overall structure of a perceptron network.

Radial basis function network: This is another type of neural network in which the output of y_j of each neuron j=1, …,p is calculated as:

$$y_j = g\left(\|X - C_j\|\right) \quad (15)$$

Where g(•) is the activation function, ‖•‖ is the Euclidean norm, X=[x_1, …,x_n] is the input vector and C_j is the center of neuron j. A commonly used activation function is the Gaussian function in the following form [24]:

$$g_j = \exp\left(-\frac{\|X-C_j\|^2}{2\sigma^2}\right) \quad (16)$$

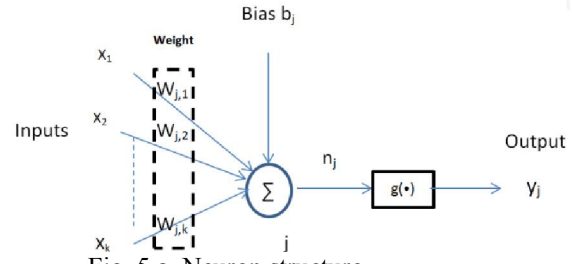

Fig. 5.a. Neuron structure

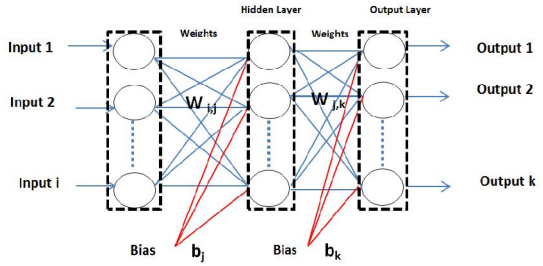

Fig. 5.b. MLP structure

3.4.Identification and training

In order to identify the models, data are acquired from the CSTH plant described in section 2. The plant is run at different operating points and 5000 data points are acquired. The first 3000 of 5000 data points are used to identify the parameters of each model and the remaining for validation purpose. The plant under study involves 5 inputs and 4 outputs yielding a 9-input 9-output model structure for the fault estimator since there are 9 parameters to be estimated.

Generally, it is difficult to identify a model using faulty data. To avoid this problem, an artificial fault vector was generated to simulate fault scenarios in each sensor, following the same strategies used in [2, 25]. Fig. 6 illustrates the fault signal used for identification. This signal is applied to train the fault estimator for input and output sensor measurements. The signal is divided into 5 parts: first a null effect is introduced to guarantee output close to zero in the absence of faults. Second abrupt variations are represented by steps. Third an incipient change is placed as a ramp. Fourth a null interval is considered again to ensure output close to zero in the absence of faults and finally white noise is included. The fault estimator can estimate any fault scenario similar to any section of the pattern shown in Fig. 6. The fault signal has unity amplitude and is duly scaled proportional to variable under analysis varying up to 50 % of the variable size.

The identification procedure is carried out by adding the signal (duly scaled) to each sensor and considering it as the output of the fault estimator. The presence of noise and disturbance in one sensor must not affect the estimation quality for other sensors. For this purpose the following iterations should be carried out for each sensor with the following characteristics: (16)

1-Considering the sensor measurements ũ(t),ỹ(t) as input for the fault estimator, adding the training pattern to the corresponding sensor and considering it as output for the fault estimator.

2-Considering the sensor measurements ũ(t),ỹ(t) as input, adding the training pattern to the corresponding sensor and random noise to other sensors and considering the pattern as output.

3-Considering the sensor measurements ũ(t),ỹ(t) as input, leaving the corresponding sensor unchanged, adding random noise to other sensors and considering a null output for the estimator.

The random noise signal δ is generated stochastically as it follows:

$$\delta(0) = 0$$
$$\delta(t) = \delta(t-1) + z \quad (17)$$

Where z has a normal distribution with unit variance and zero average. This increases the estimator robustness in the presence of noise [25-27].

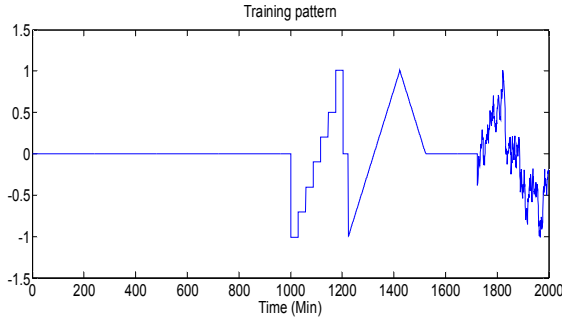

Fig. 6. Fault training pattern

for neural networks, Levenberg-Marquardt algorithm [28] is used to estimate the parameters, and normalized average quadratic error is chosen as the stopping criterion. For MLP network, 1 and 2 hidden layers each including 2-15 neurons are checked and for RBFN network, 2-25 neurons in the hidden layer are tested. For the case of Tagaki-Sugeno fuzzy model, the bell shape membership function in the following form is employed:

$$\mu_k(x) = \exp\left(-\left(\frac{x_i - c_i^k}{\sigma_k}\right)^2\right) \quad (18)$$

Where x_i is the ith input and c_i^k is the component i of vector c^k. The parameters of these functions are optimized by the gradient descent algorithm. A number of 2-25 rules are tested. Least square optimization method is applied to optimize the parameters of the output function $g^k(\bullet)$.

3.5. Training and validation analysis

Selection of the number of parameters for each model was made based on the fitting index below[21]:

$$FIT = 1 - \frac{|y-\hat{y}|}{|y-\bar{y}|} \quad (19)$$

where y is the vector that contains p measurements of the system output, $\hat{y}$ is the vector of p measurements estimated by the model, and $\bar{y}$ is a vector where all its components equals the average values of vector y.

Fig. 7 presents the results for model identification and validation as a function of parameter number. For comparison purpose, number of rules for the fuzzy model and number of hidden layers and neurons for the neural networks are varied. As it is expected the model performance improves as the number of parameters increase. However as it is shown in Fig. 7 there is an asymptotic limitation for the models. Table 2 represents the best results obtained for training and validation of the applied techniques based on the fitting index defined in equation 19 T-S fuzzy model represented the best performance; therefore it is selected as the fault estimator.

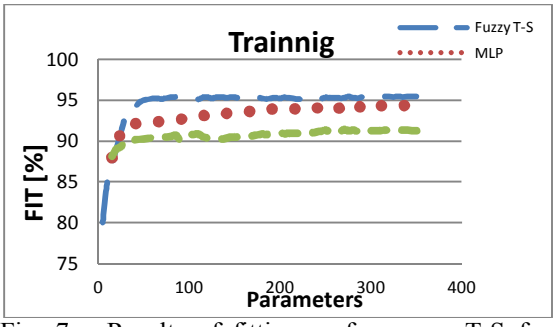

Fig. 7.a. Results of fitting performance, T-S fuzzy model showed the best performance

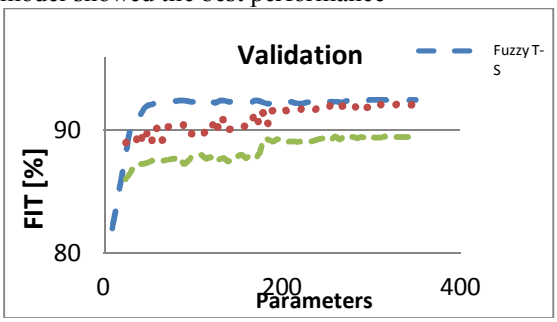

Fig. 7.b. Results of validation, T-S fuzzy model presented better validation performance

Table 2. Best obtained results for validation and training

Model	Training FIT (%)	Validation FIT (%)
T-S	95.45	91.27
MLP	94.34	91.03
RBFN	91.97	89.47

3.6. Principle Component Analysis

Principle component analysis is a statistical technique commonly used for the monitoring of the process operation. It is proposed to apply this technique in order to minimize the effects of noise and modeling error when constructing the estimator. (19)

Suppose that $X=[x_1,x_2,\ldots,x_q]$ to be a p×q matrix that contains p measurements of q symptoms delivered by the fault estimator $\left[\hat{f_u}(t), \hat{f_y}(t)\right]^T$. In order to eliminate the effect of size of each variable the following matrix is formed:

$$\bar{X} = O_s^{-1}(X - M\{X\}) \quad (20)$$

O_s is a diagonal matrix where it's elements are the variance of the variables and $E\{w\}=[m_1,m_2,\ldots,m_q]$ is the average of the variables x_i. Let C, q×q dimension matrix, be the covariance matrix of variables x_i. Decomposition of matrix Q into proper vectors corresponds to:

$$U^T C U = R \quad (21)$$

Where U is an orthonormal matrix which its columns are the eigenvectors of C and R is a diagonal matrix with eigenvalues of C.

In order to minimize the effects of noise and estimation errors, estimator output data are filtered through the k most important principle components. Let k be the number of eigenvalues of Q matrix that contain more than 99 percent of total data energy. In mathematical form it can be written as:

$$\frac{\sum_{i=1}^{k} \gamma_i}{\sum_{i=1}^{q} \gamma_i} > 0.99$$

And let $\hat{U}$ be the matrix formed by the k most important eigenvectors of matrix Q which corresponds to the k most important eigenvalues. These eigenvectors include the most important characteristics of total data set obtained from the estimator output.

Matrix $\bar{X}$ is decomposed into principle component space $\hat{X}$ and residual space $\tilde{X}$ according to the following equation:

$$\bar{X} = \hat{X} + \tilde{X}$$

$$\hat{A} = \hat{A}\bar{X} + \tilde{A}\bar{X} \quad (22)$$

Where $\hat{X}= \hat{U}\hat{U}^T$ and $\tilde{A}=1-\hat{A}$. Projection of data into the principle component space $\hat{X}$ reduces the dimension of q variables into k principle components. In the normal operating state, the residual space can is formed by subtracting the principle component

space from the normalized data $\tilde{X}= \bar{X}-\hat{X}$. In the occurrence of faults, signals cannot be interpreted by principle component space, therefore the residual space deviates from the normal operating condition and the alarm is triggered.

3.7. Fault detection (Q test)

In order to detect abrupt variations in the behavior of variables, different multivariable statistical methods are used with the principle component analysis. Hotelling test (T^2), Q test and Scheffe test are in this category [12, 28]. Since Q test is more accurate than Hotelling and Scheffe tests for classification of abnormalities [28, 29, 30] Q test is applied in this paper.

Q index or square prediction error is calculated as it follows:

$$Q = (X - \tilde{y}_f)^T (X - \tilde{y}_f) = ||\tilde{A} X||^2 \quad (23)$$

Where x is a column vector representing q variables x_i and $\tilde{y}_f$ is the prediction obtained from the principle components model. It is calculated as:

$$\tilde{y}_f = \tilde{A}X \quad (24)$$

This index shows the difference between the measurements of the variables and the predictions obtained from the principle components model.

A confidence level α can be calculated for the Q index in the following form:

$$Q_\alpha = \beta_1 \left(\frac{c_\alpha}{\beta_1} \sqrt{2\beta_2 b_0^2} + \frac{\beta_2 b_0 (b_0 - 1)}{\beta_1^2} + 1 \right)^{1/b_0} \quad (25)$$

Where:

γ_i : eigenvalue corresponding to the eigenvector u_i , column i of matrix U.

$$\beta_1 = \sum_{i=k+1}^{q} \gamma_i \quad (26)$$

$$\beta_2 = \sum_{i=k+1}^{q} \gamma_i^2 \quad (27)$$

$$\beta_3 = \sum_{i=k+1}^{q} \gamma_i^3 \quad (28)$$

$$b_0 = 1 - \frac{2\beta_1 \beta_3}{3\beta_2^2} \quad (29)$$

$$c = \beta_1 \frac{\left[\left(\frac{Q}{\beta_1} \right) - \frac{\beta_2 b_0 (b_0 - 1)}{\beta_1^2} - 1 \right]}{\sqrt{2\beta_2 b_0^2}} \quad (30)$$

It can be shown that c has approximately a normal distribution with mean zero and unit variance [31] and c_α in Equ. 16 indicates a value for which the accumulated normal distribution covers an area α.

In the presence of faults or noise, data cannot be interpreted by the principle components model. At this moment Q index exceeds Q_α threshold and the alarm is triggered. Repeated experiments indicated that the sensitivity level of the fault detection system is about 0.5% of the magnitude of variable under analysis. If faults happen in more than one sensor at the same moment (very unlikely case) or a fault happens when another fault has already occurred, Q index again will exceed the threshold and the alarm is triggered. In such situations, the fault isolation module will indicate the faulty sensors. This fault isolation module is described below.

3.8. Fault isolation

When the presence of fault is announced by the fault detection module, the faulty sensor or sensors should be isolated from those operating at normal condition. Considering the identification procedure of the fault estimator in normal operating condition, the fault estimator output should be null. However due to noise and modeling error, the estimator output shows minor deviations from zero. In the proposed scheme, this deviation is less than 1% of the magnitude of measured quantity. The maximum value of these deviations for is indicated by **DEV**. In the presence of a fault, only the part of the estimator corresponding to the faulty sensor exceeds **DEV** threshold and the faulty sensor is isolated. Therefore:

$$DEV_i = \max | \hat{f}_i(t) | \quad (31)$$

$$\hat{f}_i(t) > DEV_i \text{ For faulty sensor} \quad (32)$$

Where DEV_i is the maximum deviation from zero in the normal operating condition for the fault estimator output corresponding to ith sensor and $\hat{f}_i(t)$ is the ith estimated fault.

3.9 Signal Correction:

To reconstruct the damaged signals, all the fault estimations are subtracted from the measured signals. Faults can occur in input or output sensors [21].

If faults occur in input sensors j=1,…,m then:

$$f_{u_j}^* \neq 0 \ \forall \ j=1,2,\ldots,m \ \& \ f_{u_j}^* = 0 \ \forall \ j \neq 1,2,\ldots,m \quad (26)$$

If faults are occurred in output sensors i=1,…,n then: (27)

$$f_{y_j}^* \neq 0 \ \forall \ i=1,2,\ldots,n \ \& \ f_{y_j}^* = 0 \ \forall \ i \neq 1,2,\ldots,n \quad (28)$$

Signal reconstruction is performed as it follows: (29)

$$\begin{bmatrix} \hat{u}(t) \\ \hat{y}(t) \end{bmatrix} = \begin{bmatrix} \tilde{u}(t) \\ \tilde{y}(t) \end{bmatrix} - \begin{bmatrix} f_u^*(t) \\ f_y^*(t) \end{bmatrix} \quad (33)$$

Where $\hat{u}(t)$ and $\hat{y}(t)$ represent the the corrected signals, $\tilde{u}(t)$ and $\tilde{y}(t)$ are the sensor measurements and $f_u^*(t)$ and $f_y^*(t)$ are the estimated faults. (30)

4. Test Scenario results

In order to evaluate the system performance the following items are considered:

- Undetected faults: calculated as the percentage of time during which erroneously no fault was detected with respect to total evaluation time.
- Mean Absolute Relative Error (MARE): this value express the quality of estimated faults by fault estimator.
- Reconstruction quality: express the quality of reconstruction of the damaged signals with respect to original signal based on the fitting index defined in section 3.5.

Table 3 represents the results for fault detection for different fault scenarios . Six fault scenarios are considered and for each scenario the MARE and the undetected fault percentage is calculated. It is clear that in all the cases the undetected fault percentage is less than 4%. The maximum value for MARE is 0.0642 that indicates a satisfactory estimation quality by the fault estimator. The error of signal reconstruction is less than 6% in all the cases. Various test results indicated that the minimum detectable variation range for fault detection stage is about 0.5% of size of the variable under study and it is about 1% for fault isolation stage.

Table 3. Statistical analysis for different fault scenarios

Fault type	MARE	Not detected (%)	Corrected signal (%)
Incipient1	0.0430	2.43	94.23
Noise1	0.0384	3.12	94.79
Incipient2	0.0642	2.56	94.53
Noise2	0.0445	3.67	94.14
Abrupt1	0.0078	0.00	95.12
Abrupt2	0.0207	0.00	95.76

The fault scenarios are explicated below:

4.1. Scenario Noise 1 and noise 2

Noise faults generated by the procedure explained in section 3.4 are simulated over sensor measurements of tank2 output water flow rate and tank1 input heat rate. Because the fault signals cross the zero line several times during the, simulation interval the undetected percentage indicator rises up to approximately 4 % in this case. Fig. 8 shows the results for tank2 output water flow.

4.2. Scenario Incipient 1 and Incipient 2

Faults with incipient character are simulated over sensor measurements of the tank1 input water flow rate and tank2 output water flow rate. In this case because each fault signal crosses the zero line, there are intervals where the fault variation magnitude is less than minimum detectable threshold of the estimator. Therefore undetected intervals can be observed. As it is presented in table 3 the presence of these undetected intervals has affected the signal reconstruction quality, decreasing it about 1% comparing with the abrupt fault scenario where no undetectable intervals exist. Fig.9 demonstrates the details of this fault scenario for tank2 output water flow rate.

4.3. Scenario Abrupt 1 and Abrupt 2

Step-like faults are added to measurements of tank1 and tank2 temperature sensors. Since the minimum variation of each fault is more than the sensitivity threshold of the estimator (0.5% of the original variable size) undetected fault index is zero in this case. The maximum magnitude of each fault with respect to the original variable size is 50% and 40% respectively.

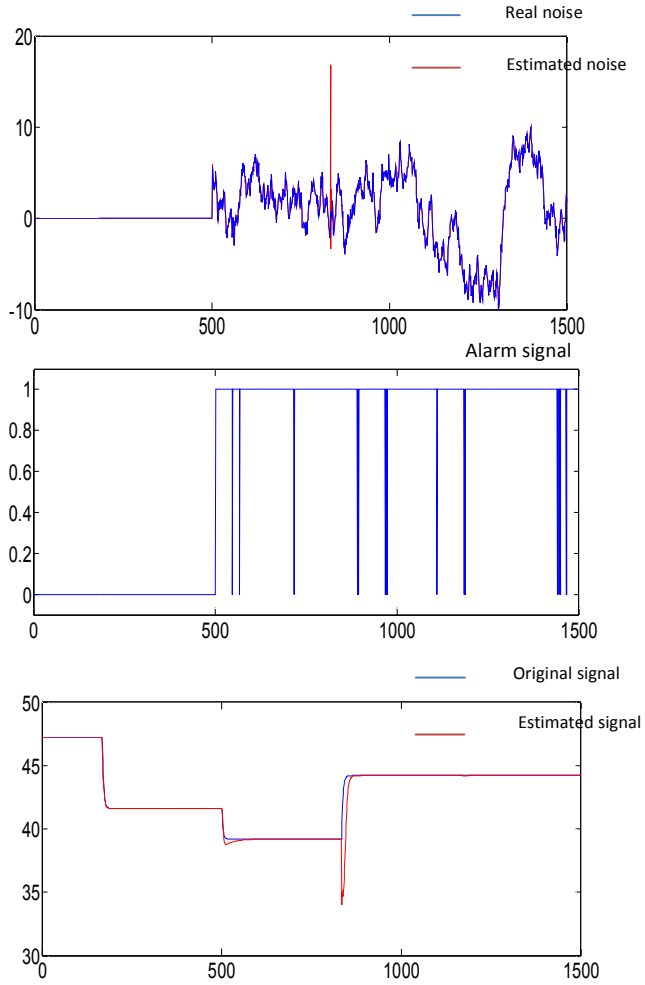

Fig. 8. Noise fault, alarm signal, original and repaired signals for tank2 output water flow.

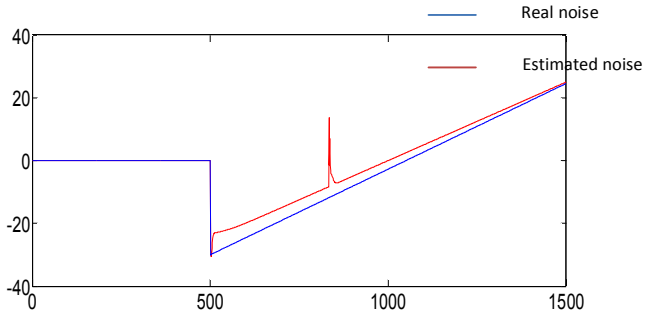

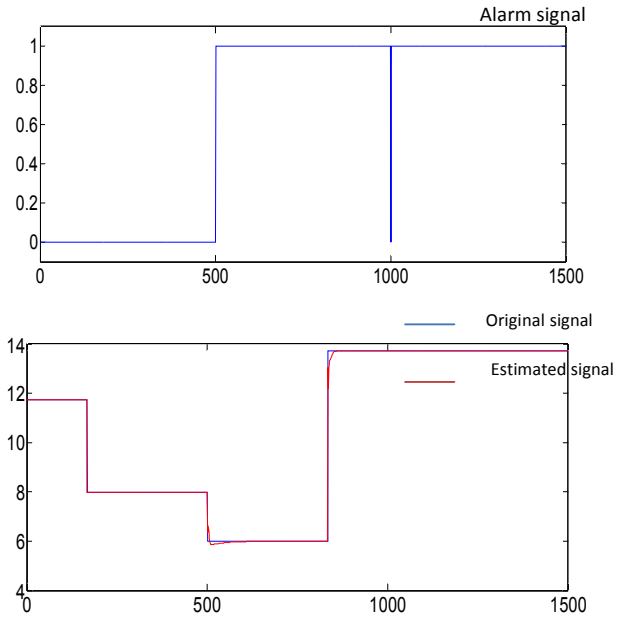

Fig. 9. Noise fault, alarm signal, original and repaired signals for tank1 input water flow rate

5. Conclusion

In this research work, a scheme is proposed for detection and isolation of multiple faults by applying dynamic modeling techniques and statistical methods. The proposed scheme was examined successfully on a CSTH model. Tagaki- Sugeno fuzzy model, Multi-layer perceptron and RBF networks were checked as the fault estimator while Tagaki- Sugeno model appeared to be the best choice. The scheme presented sufficient sensitivity for detection of faults and isolation of faulty sensors and it is capable of detecting noise, abrupt and incipient fault and repairing the damaged signal which is an important contribution from industrial viewpoint. The studied experiments showed that the percentage of undetected faults varies depending on fault character and its closeness to the sensitivity threshold. However this value had only minor effects on the quality of repaired signals since the signal correction error showed only minor degradation.

It is important to consider that the proposed scheme is independent of the process or system under study and the fault estimator has the capability of being extended to as many sensors as required, therefore the system can be generalized, trained and applied to any other process for fault diagnosis purposes.

Corresponding author:
Farouq Zargany
Department of Automation and Instrumentation
Petroleum University of Technology, Ahvaz faculty
E-mail: far.zargany@gmail.com

References:

[1] R. Dorr, F. Kratz, J. Ragot, F. Loisy, J.-L. Germain, Detection, isolation, and identification of sensor faults in nuclear power plants, IEEE Transactions on Control Systems Technology 5 (1) (1996) 42–60.

[2] S. Simani, C. Fantuzzi, R. Spina, Application of a neural network in gas turbine control sensor fault detection, in: Proceedings of the 1998, IEEE International Conference on Control Applications, vol. 1, 1998, pp. 182–186.

[3] P. Ballé, Fuzzy-model-based parity equations for fault isolation, Control Engineering Practice 7 (2) (1999) 261–270. Proceedings of American Control Conference, 2010, pp. 7016–7021.

[4] R. Raoufi, H. Marquez, Simultaneous sensor and actuator fault reconstruction and diagnosis using generalized sliding mode observers, in: Proceedings of American Control Conference, 2010, pp. 7016–7021.

[5] Z. Du, X. Jin, Tolerant control for multiple faults of sensors in VAV systems, Energy Conversion and Management 48 (3) (2007) 764–777.

[6] Nina F. Thornhill a, Sachin C. Patwardhan b, Sirish L. Shah c: A continuous stirred tank heater simulation model with applications, Journal of process control 18 (2008) 347-360.

[7]http://www.ps.ic.ac.uk/ ~ nina/CSTHSimulation/index.htm.

[8] L. Xu, H.E. Tseng, Robust model-based fault detection for a roll stability control system, IEEE Transactions on Control Systems Technology, 15 (3) (2007) 519–528.

[9] H. Sneider, P. Frank, Observer-based supervision and fault detection in robots using nonlinear and fuzzy logic residual evaluation, IEEE, Transactions on Control Systems Technology 4 (3) (1996) 274–282.

[10] E. Gómez, H. Unbehauen, P. Kortmann, S. Peters, Fault detection and diagnosis with the help of fuzzy-logic and with application to a laboratory turbogenerator, in: Proceedings of 13th IFAC World Congress, San Francisco, 1996, pp. 235–240.

[11] M. Witczak, J. Korbicz, M. Mrugalski, R. Patton, A GMDH neural network-based approach to robust fault diagnosis: application to the DAMADICS benchmark problem, Control Engineering Practice 14 (6) (2006) 671–683.

[12] L.Mendonca, J. Sousa, J.S. da Costa, An architecture for fault detection and isolation based on fuzzy methods, Expert Systems with Applications, 36 (2) (2009) 1092–1104.

[13] S. Oblak, I. Skrjanc, S. Blazic, Fault detection for nonlinear systems with uncertain parameters based on the interval fuzzy model, Engineering Applications of Artificial Intelligence 20 (4) (2007) 503–510.
[14] S. Simani, C. Fantuzzi, S. Beghelli, Diagnosis techniques for sensor faults of industrial processes, IEEE Transactions on Control Systems Technology 8 (5) (2000) 848–855.
[15] P.M. Frank, Fault diagnosis in dynamic systems using analytical and knowledge-based redundancy: a survey and some new results, Automatica 26 (3) (1990) 459–474.
[16] X. Ding, L. Guo, T. Jeinsch, A characterization of parity space and its application to robust fault detection, IEEE Transactions on Automatic Control 44 (2) (1999) 337–343.
[17] J. Gertler, Residual generation from principal component models for fault diagnosis in linear systems, in: Proceedings of the 2005 IEEE International Symposium on Intelligent Control Limassol, Cyprus, June 27–29, 2005, pp. 634–639.
[18] K. Patan, M. Witczak, J. Korbicz, Towards robustness in neural network based fault diagnosis, International Journal of Applied Mathematics and Computer Science 18 (4) (2008) 443–454.
[19] J.-H. Cho, J.-M. Lee, S. W. Choi, D. Lee, I.-B. Lee, Sensor fault identification based on kernel principal component analysis, in: Proceedings of the 2004 IEEE International Conference on Control Applications, vol. 2, 2004, pp. 1223–1228.
[20] N. Miskovic, M. Barisic, Fault detection and localization on underwater vehicle propulsion systems using principal component analysis, in: Proceedings of the IEEE International Symposium on Industrial Electronics, vol. 4, 2005, pp. 1721–1728.
[21] Rodrigo Berrios, Felipe Núñez, Aldo Cipriano, Fault tolerant measurement system based on Takagi–Sugeno fuzzy, Fuzzy Sets and Systems 174 (2011) 114–130 models for a gas turbine in a combined cycle power plant.
[22] Mohammad Shafiur Rahmana, M.M. Rashidb, M.A. Hussainc, Thermal conductivity prediction of foods by Neural Network and Fuzzy (ANFIS) modeling techniques, food and bioproducts processing, 90 (2012) 333–340
[23] K.M. Passino, S. Yurkovich, Fuzzy Control, Addison-Wesley Longman Publishing Co., Inc., Boston, MA, USA, 1997.
[24] L. Xing, D.T. Pham, Neural Networks for Identification, Prediction, and Control, Springer-Verlag New York, Inc., Secaucus, NJ, USA, 1995.
[25] S. Simani, C. Fantuzzi, Fault diagnosis in power plant using neural networks, Information Science 127 (3–4) (2000) 125–136.
[26] J. Liu, Y. Zhou, Y. Cai, J. Su, N. Zou, The application of generalized predictive control in CVT speed ratio control, in: IEEE International Conference on Automation and Logistics, 2007, pp. 649–654.
[27] D.W. Marquardt, An algorithm for least-squares estimation of nonlinear parameters, Journal of the Society for Industrial and Applied Mathematics 11 (2) (1963) 431–441.
[28] J. Jackson, A User's Guide to Principal Components (Wiley Series in Probability and Statistics), Wiley-Interscience, 2003.
[29] W. Li, H.H. Yue, S. Valle-Cervantes, S. Qin, Recursive PCA for adaptive process monitoring, Journal of Process Control 10 (2000) 471–486.
[30] G. González, M. Orchard, J. Cerda, A. Casali, G. Vallebuona, Local models for soft-sensors in a rougher flotation bank, Minerals Engineering 16 (2003) 441–453.
[31] J. Jackson, S. Mudholkar, Control procedures for residuals associated with principal component analysis, Technometrics 21 (3) (1979) 341–349.

18/1/2012